MSFC-271

Uncertainty in Tropical Ocean Latent Heat Flux Variability During the Last 25 Years

F. R. Robertson[1], H.-I. Lu[2], M. G. Bosilovich[3] and T. L. Miller[1]

Corresponding author: Franklin R. Robertson, Marshall Flight Space Center

320 Sparkman Dr, Huntsville 35805, AL, pete.robertson@nasa.gov, Tel: 256-961-7583.

Abstract

When averaged over the tropical oceans (30° N/S), latent heat flux anomalies derived from passive microwave satellite measurements as well as reanalyses and climate models driven with specified sea-surface temperatures show considerable disagreement in their decadal trends. These estimates range from virtually no trend to values over 8.4 Wm^{-2} $decade^{-1}$. Satellite estimates also tend to have a larger interannual signal related to El Nino / Southern Oscillation (ENSO) events than do reanalyses or model simulations. An analysis of wind speed and humidity going into bulk aerodynamic calculations used to derive these fluxes reveals several error sources. Among these are apparent remaining intercalibration issues affecting passive microwave satellite 10 m wind speeds and systematic biases in retrieval of near-surface humidity. Likewise, reanalyses suffer from discontinuities in availability of assimilated data that affect near surface meteorological variables. The results strongly suggest that current latent heat flux trends are overestimated.

[1] NASA / Marshall Space Flight Center, Huntsville, AL, USA.
[2] Universities Space Research Association, Huntsville, AL, USA.
[3] NASA Goddard Space Flight Center, Greenbelt, MD, USA.

1. Introduction

Latent heat flux (LHF) over the global oceans is a key climate process linking fast convective, radiative, and dynamical processes of the atmosphere to the slower, but equally dynamically active thermal reservoir below. Prospects for enhancing climate predictability from seasonal to decadal scale and beyond depend critically on an improved understanding and modeling of physical processes controlling LHF. The WMO Working Group on Air-sea Fluxes [Taylor, 2000] has articulated this need in broadest terms. The SEAFLUX project [Curry et al., 2004] has emerged as an example of focused efforts to evaluate and improve satellite-based products in particular. As a result of these efforts estimates of LHF variability on scales from interannual to decadal are now emerging. In particular, evidence for upward trends in LHF over the tropical domain has recently been reported. Chiu and Xing [2004] performed an EOF analysis on version 2 of the Goddard Satellite-based Surface Turbulent Fluxes data set (GSSTF2) and found that the leading mode exhibited an upward trend over the period 1990-2000. The structure of this mode showed positive changes in subtropical dry regions and smaller negative changes in the equatorial Pacific. Liu and Curry [2006] expanded this analysis to include reanalyses and an additional satellite algorithm, HOAPS-II (Hamburg Ocean Atmosphere Parameters and Fluxes from Space version II). Their analysis provided a similar finding of a statistically significant upward LHF trend having a similar spatial structure and they argued that surface wind speed increases were a key driver. It should be noted that the rate of LHF increase inferred from the GSSTF2 by both these studies was about 17 $Wm^{-2}dec^{-1}$, while the reanalysis estimates in Liu and Curry range from 1.6 to 8.9 $Wm^{-2}dec^{-1}$. Given the estimated climatological tropical mean LHF value of ~ 100 Wm^{-2}, variations of this magnitude demand further scrutiny. In this paper we re-examine several data sets and attempt to understand and narrow the uncertainties.

2. Data and Methodology

The analysis presented here relies on monthly means of LHF estimated through bulk aerodynamic methods as applied to satellite data and in numerical models. Two satellite-derived products are used, both of which rely heavily on Special Sensor Microwave Imager (SSM/I) radiances to provide 10m wind speeds and estimates of near surface specific humidity, q_a. For both of these data sets the fluxes were derived on daily time scales and archived as monthly mean products. HOAPS-II provides ocean turbulent flux retrievals and related quantities on several spatial and temporal scales [Schultz et al., 1997; Grassl et al., 2000; Bentamy et al., 2003]. Sea-surface temperatures (SSTs) taken from the Advanced Very High Resolution Radiometer Pathfinder data set are used to compute saturation specific humidity at the ocean surface, q_s^*. We used the monthly mean, 0.5 degree lat / lon resolution data for the period Jan. 1988 through December 2002, omitting the period July 1991 through July 1992 when aerosols from the Pinatubo eruption contaminated SST retrievals. A second data set from the University of California, Santa Barbara (UCSB) providing 0.25 degree resolution monthly mean retrievals was also used. The UCSB retrieval [Jones et al., 1999] uses a neural net methodology, training on the NOAA/PMEL TAO and Pirata buoy arrays [McPhaden, 1995] to retrieve 2m q_a (and T_a). Wind speeds for this algorithm are the version 5 retrievals of Wentz (1997). SSTs are taken from the NCEP/NCAR (National Center for Environmental Prediction / National Center for Atmospheric Research) Reanalysis [Kalnay et al., 1996].

Monthly mean fluxes and near surface meteorology were also taken from three reanalyses. These included the NCEP/NCAR Reanalysis [Kalnay et al., 1996], the NCEP-2 Reanalysis [Kanamitsu et al., 2002], and the new Japanese Meteorological Agency Reanalysis, JRA-25, [Onogi et al. 2005]. These data sets will be referred to as NN, N2, and JRA-25, respectively. The JRA-25 assimilated SSM/I column-integrated water vapor (CWV) as well as ERS-1, 2 and QuikScat scatterometer wind speeds.

However, neither the NN nor the N2 use either of these, thus providing a useful measure of independence from the other data sets. Finally, we include LHF produced by an integration of the NASA FVGCM model [Lin, 2004] forced by observed SSTs. The data are from the same integration analyzed by Bosilovich et al., [2005]. This integration is also a useful comparison because even though it is constrained by the time variation of SSTs, it is free from any time-dependent biases associated with data assimilation (e.g. the availability of SSM/I data only after July 1987). The physical parameterizations of the FVGCM are based on National Center for Atmospheric Research (NCAR) Community Climate Model version 3.0 (CCM3) physics.

3. Analysis

Our analysis focuses on tropical ocean area-averages, more specifically on departures from climatological monthly means over the base period January 1988 to December 2002. Figure 1 contains time series of LHF, $q_s^* - q_a$, and 10 m wind speed anomalies area-averaged over the tropical oceans (30^o N/S) for the data sets described above. Also shown in shading are associated SST anomalies calculated in the same fashion. Each time series has been smoothed using a 5-month running mean for presentation clarity. The LHF time series (Fig 1a) each show increases with time, although there is substantial variability, ranging from 2.6 $Wm^{-2}decade^{-1}$ for the FVGCM to 8.4 $Wm^{-2}decade^{-1}$ for UCSB. This unanimity in trend might seem impressive were it not for the fact that these values are several time larger than GPCP tropical oceanic rainfall trends (1.2 $Wm^{-2}decade^{-1}$). Since atmospheric water vapor storage is vanishingly small on these scales, there would be a large implied atmospheric transport of excess moisture to support increased precipitation over tropical land or higher latitudes. This is not apparent in the GPCP record which actually shows small rainfall decreases over land areas with time [Gu et al., 2007]. Note also that the FVGCM, though capturing much of the interannual variability associated with ENSO, has the smallest trend. While the accuracy of atmospheric model

integrations forced by observed SSTs is open to question [Wang et al., 2005], one must also question the effects of data set inhomogeneity in assimilated fields, and the accuracy of satellite-based LHF algorithms.

The origin of these differences becomes somewhat clearer when we examine time series of $q_s^* - q_a$ (Fig 1b). Of all the model runs, JRA25 shows the greatest rate of increase (0.21 g Kg^{-1} $decade^{-1}$). Part of this can be attributed to the effects of the onset of SSM/I data availability in July 1987. Relative to NN and N2 which did not assimilate SSM/I data, the JRA25 is lower by order 0.10 g Kg^{-1} before this date as compared to the four years following. It is also apparent that N2 anomalies exhibit a larger trend than NN while having similar interannual variability. Before 1995 the offset N2 anomalies are larger negative, but that after this date N2 anomalies increase to values nearly 0.10 g Kg^{-1} larger than NN. SST and, thus, q_s^* is essentially invariant between these two reanalyses. In contrast, the FVGCM integration has a much smaller $q_s^* - q_a$ trend (0.04 $Wm^{-2}decade^{-1}$).

Another interesting aspect in Fig. 1b is the distinctly larger magnitude of $q_s^* - q_a$ anomalies in the two satellite-based algorithms during ENSO events compared to those in the reanalyses. We believe that this stems from the inability of satellite algorithms to discern systematic variations in the relationship of near-surface moisture in the planetary boundary layer (PBL) with that of CWV. This issue was first noted in a climatological sense by Esbensen et al. [1993] who found that Liu's (1986) method of retrieving q_a from CWV yielded systematic underestimates of q_a in subsiding trade wind regimes and over-estimates in zones of convergence and deep convection. In the subtropics, mean tropospheric subsidence in the atmospheric column dries the column by vertical advection. However, in the well-mixed lower portion of the PBL, the *fractional* reduction in moisture is not as pronounced as in the free troposphere. In regions of anomalous ascent, vertical pumping of moisture provides a larger *fractional* elevation of free-tropospheric moisture than occurs near the surface. To see if this effect is

modulated by ENSO we constructed satellite minus NN q_a anomalies and composited them for both El Nino and La Nina years. By further differencing the La Nina from the El Nino composites (e.g. warm SST versus cold SST years) we see systematic patterns of q_a bias in UCSB or HOAPS q_a relative to NN (Fig. 2a,b). Overestimates in the central equatorial Pacific during El Nino are surrounded by underestimates to the west and over the adjacent subtropics. This pattern corresponds to anomalous upward motion in the equatorial eastern Pacific and sinking motion in the surrounding areas. Bias values are more prominent in HOAPS than in UCSB. The effects of widespread tropospheric sinking during warm events dominates the area average value in both data sets, leading to overestimates of q_s^* - q_a and, thus, LHF anomalies. The opposite situation holds during ENSO cold events (e.g. 1999-2000).

Another way of looking at this issue is to compare the relative variations of CWV and q_a from reanalyses during ENSO events. All q_a estimates based on satellite passive microwave rely essentially on the CWV signal either explicitly or implicitly. Thus, for consistency with the bias mechanisms outlined above we would expect that true fractional CWV variations are larger than those of true q_a. Using NN data we composited anomalies of $\log_{10}$ CWV and $\log_{10}$ q_a for El Nino and La Nina events, subtracting the La Nina composite from the El Nino composite. The results (Fig 2c,d) indeed show that compared to q_a, fractional increases in CWV are larger positive over the equatorial Pacific and larger negative over subsidence regions in the subtropics and Maritime Continent. This is not a result peculiar to NN, the same results were obtained when we used the FVGCM which is independent of any data assimilation uncertainties. On the basis of these results we conclude that the pronounced variations in q_s^* - q_a for the satellite data sets (Fig 1b) are likely exaggerated, as are interannual variations in LHF (Fig 1a) that they support.

Figure 1c compares monthly wind speed anomalies (computed from daily wind speeds). The magnitudes of these departures are several tenths of m s^{-1} corresponding to order 5% departures from

climatological values. NN and N2 anomalies track very closely, perhaps because assimilated dynamical fields are more strongly shielded from model physics changes than are quantities such as near-surface moisture. Likewise, JRA-25 tracks NN and N2 before 1995, but then decreases for several years before suddenly rising sharply in 2001. Mid-1995 marks the onset of Environmental Research Satellite (ERS-1, 2) scatterometer wind assimilation by JRA-25. QuikScat winds are assimilated beginning in mid-1999 and are the only scatterometer winds after ERS-2 ceases in 2001. It is possible that rain and cloud contaminated wind retrievals may still not be adequately flagged in these data sets and are having a systematic effect. Interestingly, the FVGCM wind speeds have little coherence with reanalysis winds on short time scales associated with transient climate "noise" but seem to capture lower frequency behavior such as elevated speeds in the late 1980s and lower values in the early 1990s. They also show no signs of the JRA-25 wind speed drop and subsequent rise beginning in 1995.

Perhaps the most surprising aspect of Fig.1c is the large variability and trend associated with the two SSM/I wind time series. These algorithms are independent from each other yet agree closely in their departures from assimilated wind speeds. Here too it is possible that liquid water is contaminating wind retrievals, but satellite intercalibration seems a more likely explanation. The agreement of high frequency interannual SSM/I variations with assimilated wind speeds (e.g. the mid-1990s) and the presence of step-like departures at the end of 1992 and 1997 support this argument. Wentz et al., [2007] have recently shown that intercalibration improvements in the new version 6 of the SSM/I products greatly reduce this trend in SSM/I surface wind speeds and substantially reduce inferred LHF estimates.

4. Discussion

From this comparison of LHF data sets on interannual to decadal scales there clearly exist uncertainties in current data sets that rival interannual to decadal signals. The most prominent distinction is between satellite-based and reanalysis LHF estimates. The former appear to have significant explainable biases in q_s^*-q_a on ENSO time scales, and the wind speeds have significant departures from assimilated fields suggestive of sensor intercalibration issues. The latter drive large upward temporal trends in the satellite LHF. The GSSTF2 data set analyzed by Liu and Curry [2006] has an even larger trend (~17 $Wm^{-2}decade^{-1}$) due in part to use of the earlier version 4 of SSM/I wind and CWV products. The reanalysis with the largest trend, JRA-25, owes part of this behavior to non-uniform temporal extent of assimilated data sets, most notably, onset of SSM/I availability in 1987 and the use of scatterometer winds beginning in 1995. These results do not, however, suggest that NN and N2 should be regarded as definitive since there are many known deficiencies in these and other reanalyses. We have purposely excluded the 40-year European Center Reanalysis, ERA-40, because of satellite radiance calibration and water vapor assimilation issues which have led to known biases in hydrologic cycle processes [Bengtsson et al., 2004; Andersson et al, 2005]. It appears also that blended products using satellite, reanalysis, and buoys cannot fully resolve the issues found here. Yu and Weller [2007] report an increase of about 9 Wm^{-2} *globally* during the period 1981 to 2002 for their Objectively Analyzed Air-sea Heat fluxes (OAFlux) data set. However, the GSSTF2 q_a estimates and winds taken from version 4 of the Wentz SSM/I products are integral components of this analysis and likely contribute to a spurious upward trend.

We would argue that given the error sources identified in the present results, the degree to which interannual variations in LHF at regional scales integrate to a discernable tropic-wide trend remains an open question. In terms of long-term greenhouse gas forcing effects, Held and Soden [2006] argue for a scaling of order 2% rise in precipitation (or evaporation) per degree SST rise which, given the ~.17 K SST rise over the tropical oceans during the past 25 years, would yield a LHF increase of order 0.5

Wm^{-2}. This is far smaller than variations noted in the present results. However, there do exist candidate physical mechanisms for producing variations of decadal scale and longer. Among these are possible reddening of the ocean upper ocean heat content variations by "higher frequency" ENSO events similar to that hypothesized by Newman et al., [2003] or low-frequency variations in the shallow meridional overturning circulation of the Pacific Ocean [McPhaden and Zhang, 2004]. Associated ocean heat transports would likely lead to subsequent adjustments with the overlying atmosphere through surface fluxes.

It is expected that ongoing improvements to existing data sets [e.g. Wentz et al., 2007] and planned reanalyses (e.g. the NASA Modern-Era Retrospective Analysis for Research and Applications) will substantially improve prospects for isolating physical signals of LHF variations.

References

Andersson, E. et al. (2005), Assimilation and modeling of the atmospheric hydrological cycle in the ECMWF forecasting system . *Bull. Amer. Meteor. Soc.,* 86,(3), 387–402.

Bengtsson, L., S. Hagemann and K Hodges (2004), Can climate trends be calculated from reanalysis data? *J. Geophys. Res.*, *109*, D11111, doi:10.1029/2004JD004536.

Bentamy A., K. B. Katsaros, A. M. Mestas-Nuñez, W. M. Drennan, E. B. Forde, and H. Roquet (2003), Satellite estimates of wind speed and latent heat flux over the global oceans. *J. Climate*, *16*, 637-656.

Bosilovich, M. G., S. D. Schubert, and G. K. Walker (2005), Global changes of the water cycle intensity, *J. Clim., 18*, 1591-1608.

Chiu, L.S. and Y. Xing (2004), Modes of interannual variability of oceanic evaporation observed from GSSTF2. *Int. J. Biodiversity,Oceanology and Conservation*, *68*, (2), 115-120.

Curry, J. A., et al. (2004), SEAFLUX, *Bull. Am. Meteorol. Soc., 85*, 409–424.

Esbensen, S. K., D. B. Chelton, D. Vockers, and J. Sun (1994), An analysis of errors in Special Sensor Microwave Imager evaporation estimates over the global oceans. *J. Geophy. Res.*, *98*, 7081-7101.

Grassl, H., V. Jost, R. Kumar, J. Schulz, P. Bauer, and P. Schluessel (2000), *The Hamburg Ocean-Atmosphere Parameteres and Fluxes from Satellite Data (HOAPS): A Climatological Atlas of Satellite-Derived Air-Sea-Interaction Parameters over the Oceans.* Report No. 312, ISSN 0937-1060, Max Planck Institute for Meteorology, Hamburg.

Gu, G., R. Adler, G. Huffman, and S. Curtis (2007), Tropical rainfall variability on interannual-to-interdecadal/longer-time scales derived from the GPCP monthly product, *J. Climate*, (in press).

Held, I. M., and B. J. Soden (2006), Robust responses of the hydrological cycle to global warming, *J. Climate, 19,* 5686–5699.

Jones, C., P. Peterson, and C. Gautier (1999) A new method for deriving ocean surface specific humidity and air temperature: an artificial neural network approach. *J. Appl. Meteor., 38*, 1229–1246.

Kalnay, E., et al. (1996), The NCEP/NCAR 40-year Reanalysis Project. *Bull. Amer. Meteor. Soc., 77*, 437–471.

Lin, S.-J. (2004), A "vertically Lagrangian" finite-volume dynamical core for global models. *Mon. Wea. Rev., 132*, 2293–2307.

Liu, W. T. (1986), Statistical relation between monthly mean precipitable water and surface-level humidity over global oceans. *Mon. Wea. Rev., 114*, 1591-1602.

Liu, J., and J. A. Curry (2006), Variability of the tropical and subtropical ocean surface latent heat flux during 1989–2000, *Geophys. Res. Lett. 33,* L05706, doi:10.1029/2005GL024809, 2006.

Kanamitsu, M., W. Ebisuzaki, J. Woolen, J. Potter, and M. Fiorino (2002), NCEP/DOE AMIP-II reanalysis (R-2), *Bull. Amer. Meteor. Soc., 83*, 1631– 1643.

McPhaden, M. J. (1995), The tropical atmosphere ocean array is completed. *Bull. Amer. Meteor. Soc., 76*, 739-742.

McPhaden M. J. and D. Zhang (2004), Pacific Ocean circulation rebounds, *Geophys. Res. Lett., 31*, L18301, doi:10.1029/2004GL020727.

Newman, M., G. P. Compo, and M. A. Alexander (2003), ENSO-forced variability of the Pacific Decadal Oscillation, *J. Clim., 16*, 3853-3857.

Schulz, J., J. Meywerk, S. Ewald, and P. Schluessel (1997), Evaluation of satellite-derived latent heat fluxes. *J. Climate, 10*, 2782-2795.

Onogi and co-authors (2005), JRA-25 Japanese 25-year re-analysis project—progress and status. *Q. J. R. Meteorol. Soc., 131*, 3259–3268.

Taylor, P.K., 2000: Intercomparison and validation of ocean-atmosphere energy flux fields. Final report of the Joint WCRP/SCOR Working Group on Air-Sea Fluxes,WMO/TD-No. 1036, Geneva, Switzerland

Wang, B., Q. Ding, X. Fu, I.-S. Kang, K. Jin, J. Shukla, and F. Doblas-Reyes (2005), Fundamental challenge in simulation and prediction of summer monsoon rainfall. *Geophys. Res. Lett.*, *32*, L15711, doi:10.1029/2005GL022734.

Wentz, F.J. (1997), A well calibrated ocean algorithm for special sensor microwave/imager, *J. Geophys. Res., 102(C4)*:8703-8718.

Wentz F. J., L. Ricciardulli, K. Hilburn and Carl Mears (2007), How much more rain will global warming bring? *Science* DOI: 10.1126/science.1140746

Yu, L., and R. A. Weller (2007), Objectively analyzed air-sea heat fluxes for the global ice-free oceans (1981-2005), *Bull. Am. Meteor. Soc., 88*,527-539.

Figure Captions

Figure 1. Anomaly time series for LHF, q_s^*-q_a, and 10m wind speed for NN (black), N2 (black dot), JRA-25 (blue), FVGCM (gold), HOAPS II (green) and UCSB (red). Anomalies are with respect to 1988-2002 mean annual cycle (except FVGCM, 1988-1998). SST anomalies are shaded gray. FVGCM wind speeds are only available through 1998.

Figure 2. Anomalies of (a) q_a (UCSB minus NN) and (b) q_a (HOAPS II minus NN) for El Nino minus La Nina composites with units of g Kg^{-1}; (c) fractional anomalies (dimensionless) of $\log_{10}$ CWV and (d) $\log_{10}$ q_a for El Nino minus La Nina composites made from NN reanalysis data.

Acknowledgements

This research was conducted under support from the NASA Energy and Water Cycle Study, Dr. Jared Entin, Program Manager. Dan Fitzjarrald and Jayanthi Srikishen provided programming support.

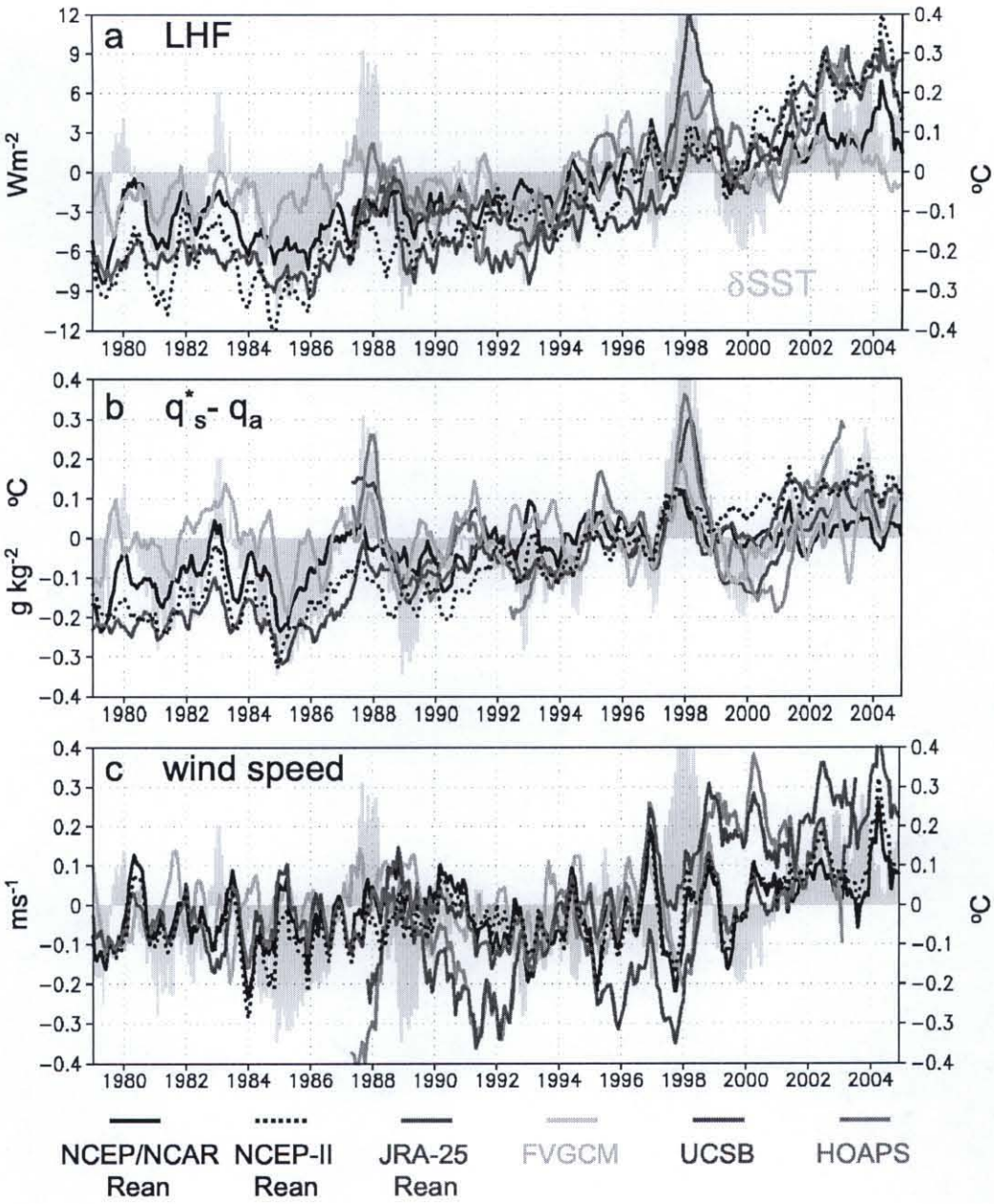
a LHF
Wm-2
°C
δSST
b q*s- qa
g kg-2
°C
c wind speed
ms-1
°C
1980 1982 1984 1986 1988 1990 1992 1994 1996 1998 2000 2002 2004
NCEP/NCAR Rean
NCEP-II Rean
JRA-25 Rean
FVGCM
UCSB
HOAPS

Figure 1

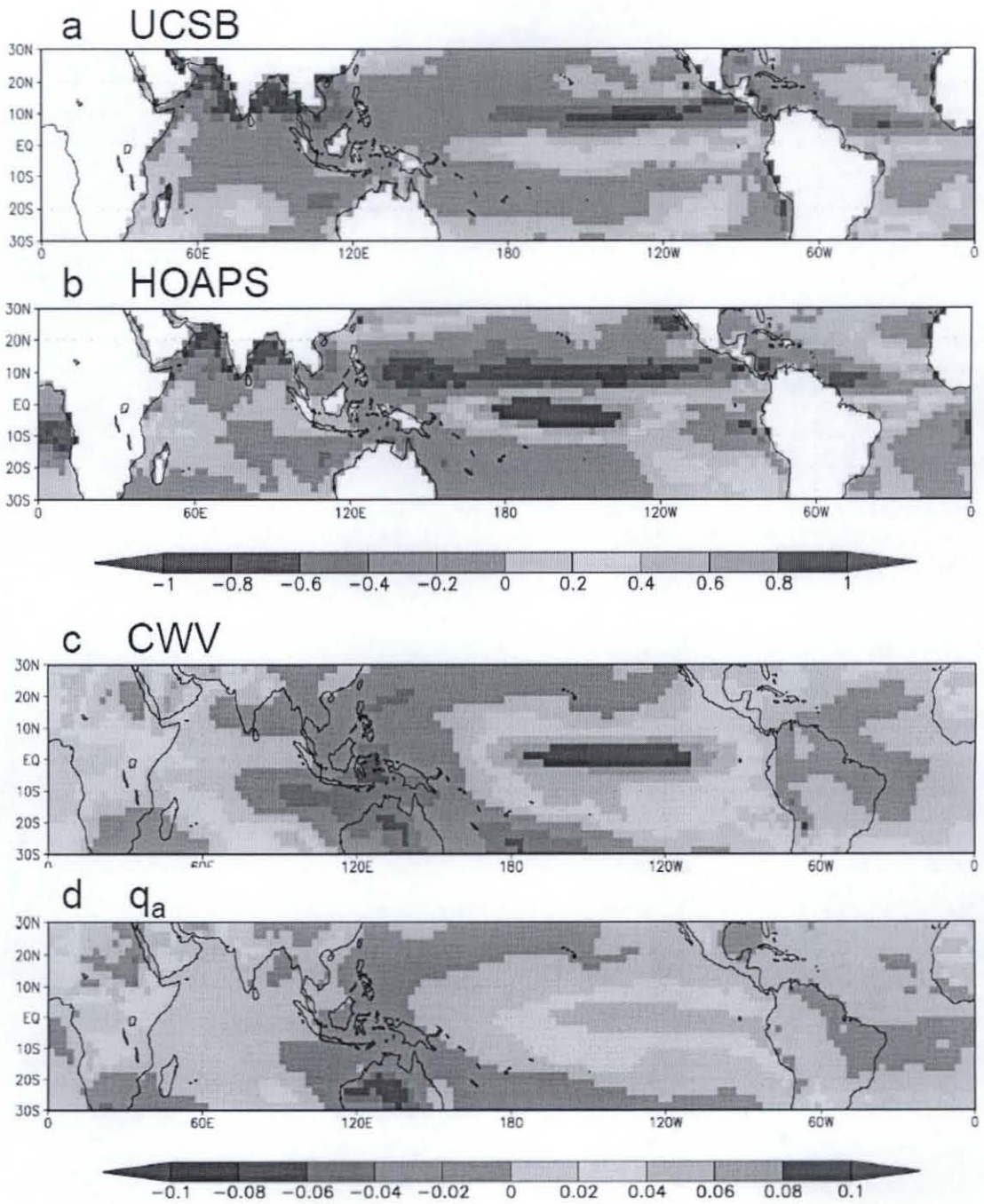
a UCSB
b HOAPS
c CWV
d q_a
30N
20N
10N
EQ
10S
20S
30S
0
60E
120E
180
120W
60W
−1 −0.8 −0.6 −0.4 −0.2 0 0.2 0.4 0.6 0.8 1
−0.1 −0.08 −0.06 −0.04 −0.02 0 0.02 0.04 0.06 0.08 0.1

Figure 2